

Solitonic-exchange mechanism of surface diffusion

Oleg M. Braun,* Thierry Dauxois,[†] and Michel Peyrard

Laboratoire de Physique de l'École Normale Supérieure de Lyon, 46 Allée d'Italie, 69364 Lyon Cédex 07, France

(Received 28 November 1995)

We study surface diffusion in the framework of a generalized Frenkel-Kontorova model with a nonconvex transverse degree of freedom. The model describes a lattice of atoms with a given concentration interacting by Morse-type forces, the lattice being subjected to a two-dimensional substrate potential which is periodic in one direction and nonconvex (Morse) in the transverse direction. The results are used to describe the complicated exchange-mediated diffusion mechanism recently observed in molecular dynamics simulations [J. E. Black and Zeng-Ju Tian, *Phys. Rev. Lett.* **71**, 2445 (1993)]. [S0163-1829(96)00726-6]

I. INTRODUCTION

Diffusion of atoms adsorbed on crystal surfaces is important in many processes such as surface reactions and crystal growth of artificially layered materials.^{1,2} In addition, surface diffusion is of considerable intrinsic interest, because experimental results show a very rich and complicated behavior of diffusion coefficients, especially as a function of the atomic concentration.

When the first adsorbed layer is complete, new incoming atoms start to fill the second adlayer. Usually the diffusion in the second layer follows the same laws as that in the first layer because the adatoms of the first monolayer play the role that substrate atoms played for the diffusion of the adatoms of the first layer, i.e., the first-layer adatoms create an external potential for the second-layer atoms. However, for some adsystems the situation may be more complicated owing to exchange of atoms between the first and second adlayers. Such an exchange was observed experimentally by Medvedev *et al.*³ for the Li-W(112) and Li-Mo(112) adsystems, where the growth of the second layer results in the reconstruction of the underlying first adlayer. Moreover, recently Black and Tian⁵ have observed a "complicated exchange-mediated diffusion mechanism" in a molecular dynamics experiment, where an isolated Cu adatom, which is diffusing on the Cu(100) surface, may enter the first substrate layer and create there a strain along a close-packed row. This localized excitation moves along the row for a distance of several lattice constants, and then the strain is relieved by an atom in the strained row popping out and returning to the surface. The simulation showed that this diffusion mechanism becomes important at high enough temperatures [$T \sim 900$ K for the Cu-Cu(100) adsystem].

The effect of reconstructive crystal growth was studied theoretically in Ref. 6 within the framework of a generalized Frenkel-Kontorova (GFK) model with a nonconvex transverse degree of freedom. The model describes a chain of atoms interacting with a generalized Morse potential. The atoms are assumed to be mobile in two directions, one along the surface (this is the direction along which the atoms can diffuse), and the other one orthogonal to the surface. They are subjected to a two-dimensional substrate potential which is periodic along the chain (i.e., along the surface) and has the shape of a Morse potential in the transverse direction

(orthogonal to the surface). The concentration of atoms is characterized by the dimensionless parameter $\theta = N/M$, the so-called coverage in surface physics, where N is the number of atoms and M is the number of minima of the external potential. This model may be considered as a "minimal" model which takes into account all main features of real adsorbed systems such as layers adsorbed on furrowed crystal surfaces. On the other hand, it is simple enough to be tractable analytically, at least in some aspects. The aim of the present paper is to show that the same model⁶ can provide a useful framework to study the role of the atomic exchange between the first and second adlayers in surface diffusion at coverages $\theta \gtrsim 1$.

In the study of surface reconstruction,⁶ it has already been shown that the formation of a metastable defect (kink) in which an atom of the second layer penetrates into the first layer is possible in some parameter range of the GFK model. As kinks of the first layer generally have a diffusion coefficient D_k which is much larger than the diffusion coefficient D_{act} of thermally activated atoms of the second layer, it was speculated that the formation of such defects could have a large influence on the overall diffusion of atoms on crystal surfaces. The present work confirms this conjecture and provides quantitative evaluations of the role of this exchange-solitonic mechanism on surface diffusion. We study a system of adsorbed atoms which has a complete first adlayer and an extra adatom that can be in two stable configurations. In the first one, the extra atom is in the second layer. This state corresponds to the minimum of the total potential energy (the gs configuration). The second configuration with all adatoms in the first layer corresponds to a metastable state (the ms configuration). In this ms configuration the extra atom creates a localized solitonic excitation, the so-called kink, which usually has a very high mobility. Thus, even if the lifetime of the ms configuration is small at a nonzero temperature, the ms configuration may play the main role in surface diffusion, generating an unusual temperature dependence of the mass diffusion coefficient.

The paper is organized as follows. The model is described in Sec. II. Calculations of quasiadiabatic trajectories are described in Sec. III, and the results of molecular dynamics simulation are presented in Sec. IV. Section V is devoted to theoretical estimations of different diffusion mechanisms. The last section, VI, concludes the paper.

II. MODEL

We use the generalized Frenkel-Kontorova model introduced in Ref. 6. The displacement of an atom is characterized by two variables: x describes its motion parallel to the surface and y describes its deviation orthogonal to the substrate. The potential perpendicular to the surface has a Morse shape,

$$V_y(y) = \varepsilon_d (e^{-\gamma y} - 1)^2, \quad (1)$$

which tends to the finite limit ε_d (known as the adsorption energy) when $y \rightarrow \infty$. The parameter γ determines the anharmonicity and it is related to the frequency ω_y of a single-atom vibration in the normal direction by the relation $\omega_y^2 = 2\gamma^2 \varepsilon_d / m$, m being the atomic mass. It should be noticed that the function (1) is nonconvex, i.e., it has an inflection point at $y = y_{\text{inf}} \equiv \gamma^{-1} \ln 2$, which has important consequences on the properties of the system.⁶ To model the substrate potential along the surface, we use the deformable periodic potential⁷

$$V_x(x) = \frac{1}{2} \varepsilon_s \frac{(1+s)^2 [1 - \cos(2\pi x/a_s)]}{1+s^2 - 2s \cos(2\pi x/a_s)} \quad (2)$$

as discussed in previous work.⁸ Here ε_s is the activation energy for diffusion of a single atom, a_s is the period of the substrate potential along the chain, and the parameter s ($|s| < 1$) determines the shape of the potential. The frequency ω_x of a single-atom vibration along the chain is connected to the shape parameter s by $\omega_x^2 = \omega_0^2 [(1+s)/(1-s)]^2$ with $\omega_0^2 \equiv 2\pi^2 \varepsilon_s / m a_s^2$. In the following we use a system of units where $a_s = 2\pi$, $\varepsilon_s = 2$, and $m = 1$, so that $\omega_0 = 1$.

The total potential energy of a single atom interacting with the substrate is written as

$$V_{\text{sub}}(x, y) = V_x(x) e^{-\gamma' y} + V_y(y). \quad (3)$$

The exponential factor in the first term of the right-hand side of Eq. (3) takes into account the decrease of the influence of the surface corrugation as the atoms move away from the surface, so that $V_{\text{sub}}(x, y) \rightarrow \varepsilon_d$ when $y \rightarrow \infty$.

To model the interaction between adatoms, we use the generalized Morse potential

$$V_{\text{int}}(r) = \varepsilon_a \left\{ \frac{\beta'}{\beta - \beta'} e^{-\beta(r-r_a)} - \frac{\beta}{\beta - \beta'} e^{-\beta'(r-r_a)} \right\}, \quad (4)$$

where ε_a is the interatomic bonding energy of a molecule adsorbed on the surface, r_a is the molecule's equilibrium distance, and the exponents β and β' are related to the frequency ω_a of interatomic vibration by the relation $\omega_a^2 = \varepsilon_a \beta \beta'$.

We use the same model parameters as in the study of surface reconstruction, Ref. 6; namely, considering the case of metal atoms adsorbed on a metal substrate such as, e.g., the Li-W(112) or the Li-Mo(112) adsystems, we take $a_s = 2.73 \text{ \AA}$ which is the distance between the wells along a furrow on the W(112) surface, and $\varepsilon_s \sim 0.1 \text{ eV}$, $\varepsilon_d \sim 3 \text{ eV}$, $\omega_x \lesssim \omega_y \sim 10^3 \text{ cm}^{-1}$, which are typical values for these systems. Returning to our system of units, we get $\varepsilon_d = 60$, $\gamma = 0.183$, $y_{\text{inf}} = 3.80$, $\omega_x = 1.5$, $\omega_y = 2$, $\gamma' = 2\gamma = 0.366$, and

$s = 0.2$. The interaction energy between two adsorbed metal atoms usually lies within an interval $\varepsilon_a \sim 0.1 - 0.5 \text{ eV}$,¹⁰ or $\varepsilon_a \sim 2 - 10$ in our system of units; we have chosen the value $\varepsilon_a = 6$. For the exponents β and β' we take $\beta = 1.9$ and $\beta' = 0.19$ (see a more detailed discussion of such a parameter choice in Ref. 6). In Ref. 6 we had chosen for the interatomic equilibrium distance the value $r_a \approx 3.04 \text{ \AA}$ (the interatomic distance in lithium metal), or $r_a = 7$ in our system of units, because we had in mind the application of the model to the lithium film. However, we will use in the present work lower values of r_a , $r_a = 6.3$ and 6.4 , in order to investigate the case when an extra atom can be inserted into the first adlayer and exist there in a metastable state. Although we have selected some of the parameters by comparison with a real system, we do not claim to describe quantitatively a concrete system of adatoms with a model which is still oversimplified. We are interested in the *phenomenon* of exchange-mediated diffusion, and this is why the parameter r_a has been adjusted to allow such a phenomenon.

In the present work we study the case of a fixed concentration of atoms. Therefore we impose periodic boundary conditions with a fixed number M of minima of the substrate potential as well as a fixed number N of adatoms (we have used $M = 16$ and $N = 17$). The ground state configuration as well as the nearest metastable states are searched for with a standard molecular dynamics (MD) algorithm; namely, we start from an appropriate initial configuration and allow the atoms to relax to the nearest minimum of the total potential energy of the system. Thus the computer algorithm reduces to the solution of the equations of motion which follow from the potentials (3) and (4) with an artificially introduced viscous friction.^{9,6} In computer simulations we can only include the interaction with a finite number of neighbors. This is achieved by introducing a cutoff distance r^* (we have chosen $r^* = 5.5 a_s$) and accounting only for the interactions between the atoms separated by distances lower than r^* , as usual in MD simulation.

III. QUASIADIABATIC TRAJECTORIES

Adiabatic characteristics of the system were studied in order to determine the potential energy surface of the model. First, we have determined the ground state with the MD algorithm with friction, in the same way as in the study of surface reconstruction.⁶ Then, in order to investigate mass diffusion, we have investigated the dependence of the potential energy upon the position of the center of mass of the system. It is, however, difficult to impose a constraint on the center of mass. Therefore, instead of determining this adiabatic trajectory, we explore the multidimensional potential energy surface along "quasiadiabatic" trajectories defined by imposing appropriate constraints on a single atom. The most important characteristics of the motion, which are the positions and energies of the stationary points (the ground state, the metastable state, and the saddle points), are calculated correctly by this method, and we may expect to obtain the correct shape of the adiabatic trajectory at least qualitatively with this approach.

Since we consider the possibility that the extra atom may exist in two stable states that differ by its distance to the substrate (atom in the second or in the first layer), a first

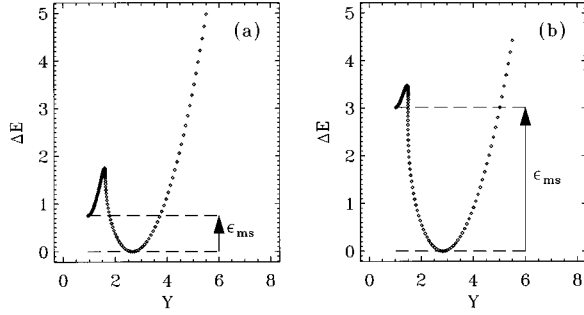


FIG. 1. Change of energy ΔE with respect to the ground state as a function of Y for a displacement along the quasiadiabatic trajectory perpendicular to the surface for (a) $r_a = 6.3$ and (b) $r_a = 6.4$.

analysis has been performed by constraining only the y coordinate y_j of the extra atom. We displace it up and down in the y direction (perpendicular to the surface) by small steps. At each step we allow for the x coordinate of this atom and for both coordinates of all other atoms to adjust themselves to the new value of y_j . For each relaxed state, the position Y of the center of mass of the system is calculated. Figure 1 shows the dependence of the system energy upon Y . The ground state configuration corresponds to a Y position of the kink around 2.8, while the metastable state corresponds to a much lower value of Y . These pictures allow us to calculate ε_{ms} , the difference in energies of the metastable and ground states. The results are listed in Table I. One can notice that ε_{ms} depends very much on r_a ; the metastable state is much more likely to be relevant in the case (a) $r_a = 6.3$ which has a lower ε_{ms} than in case (b) $r_a = 6.4$. The two stable states are separated by a barrier $\varepsilon_{barrier}$.

Around each value of Y corresponding to a stable state, we have then determined the potential energy as a function of the displacement along x of the coordinate x_j of the extra atom. In this case x_j is constrained to a given value but y_j is allowed to relax to its equilibrium value as well as the x and y coordinates of all the other atoms. The X coordinate of the center of mass is again calculated for each relaxed state. The results are presented in Fig. 2 for the case of a quasiadiabatic trajectory starting from the ground state, and in Fig. 3 for a trajectory starting from the metastable state. In this case, the structure of the metastable defect is such that the extra atom does not play a specific role and cannot be identified unambiguously. This has no consequence on the mass diffusion,

TABLE I. Parameters of quasiadiabatic trajectories for two values of the equilibrium distance r_a of the interatomic potential. ε_{ms} is the difference in energies of the metastable and ground state configurations, $\varepsilon_{barrier}$ is the activation barrier for the transition from the gs configuration to the metastable state, ε_{act} is the activation energy for the hopping diffusion, and ε_{PN} is the barrier for kink motion parallel to the surface.

Parameter	$r_a = 6.3$	$r_a = 6.4$
ε_{ms}	0.755	3.014
$\varepsilon_{barrier}$	1.752	3.476
ε_{ac}	2.364	2.055
ε_{PN}	4.18×10^{-6}	6.39×10^{-6}

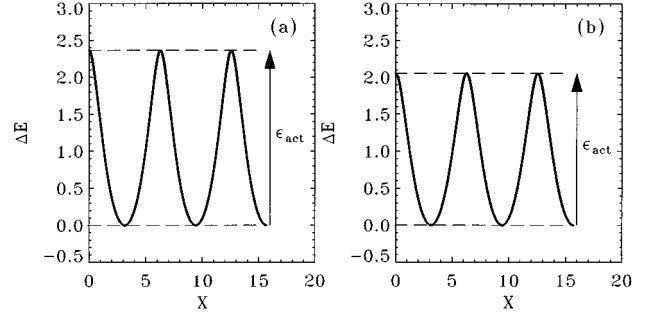


FIG. 2. Change of energy ΔE with respect to the ground state as a function of X for a quasiadiabatic displacement parallel to the surface starting from the ground state for (a) $r_a = 6.3$ and (b) $r_a = 6.4$.

but in the algorithm one has to choose the atom that will be constrained to a given x_j . The choice has been done in the same way as in Ref. 9. Figure 2 shows that, for the translation of the center of mass along x in the case of an extra atom in the second layer, there is no metastable state and only a barrier to overcome. The diffusion in the X direction will therefore be an activated process and we call ε_{act} the difference between the unstable maximum state and the stable one. As attested by the results presented in Table I, ε_{act} decreases when r_a increases. More precise consequences for the physics will be explained in the following section. Figure 3 and Table I show that the barrier ε_{PN} for the X translation of the metastable state is extremely low compared to ε_{act} .

In order to complete the picture of the potential energy surface, in a second series of calculations we artificially moved the same atom j , but now both coordinates x_j and y_j were constrained, while the other atoms were allowed to relax to the minimum of the system energy. The atom j was moved to scan the x and y directions as in a TV sweep. The results allow us to draw the full picture of the energy E of the system as a function of X and Y . They are presented in Fig. 4(a) as a contour map and in Fig. 4(b) as a three-dimensional surface (we show the results only for $r_a = 6.3$, because the case $r_a = 6.4$ looks qualitatively similar).

From the energy surface of Fig. 4 and the quantitative results of Table I, one can predict the general behavior of the

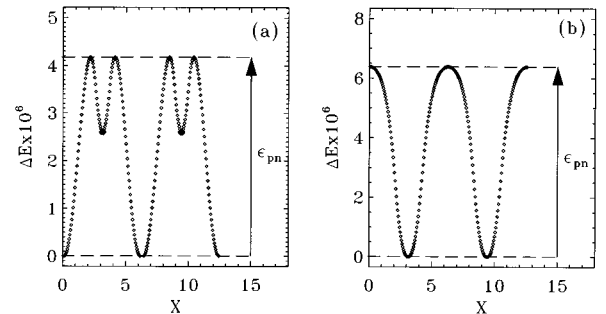


FIG. 3. Change of energy ΔE as a function of X for a quasiadiabatic displacement parallel to the surface starting from the metastable state for (a) $r_a = 6.3$ and (b) $r_a = 6.4$.

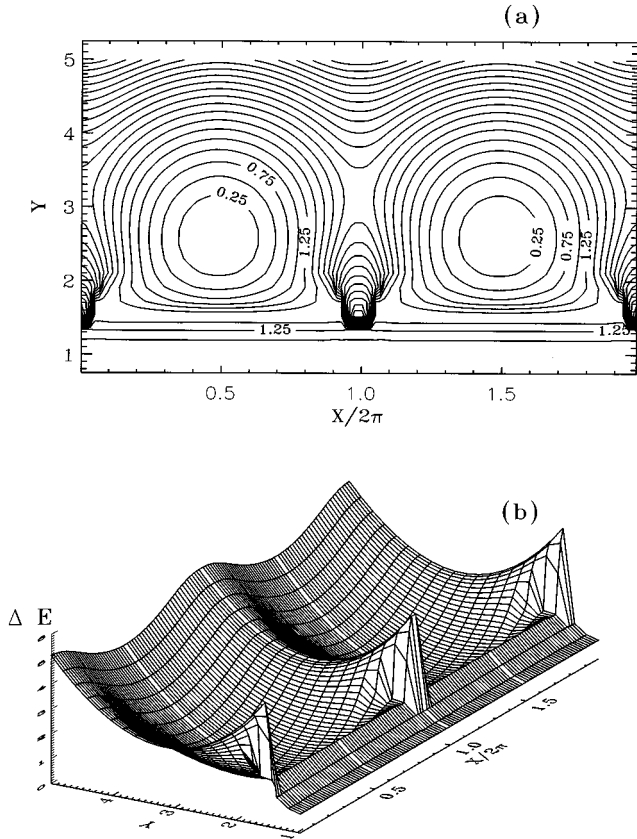


FIG. 4. Potential energy surface for the case $r_a = 6.3$. The X - Y contour map is plotted in (a) while (b) presents a three-dimensional plot.

system. Starting from the ground state in the second layer, the extra adatom may overcome the barrier ε_{act} and directly jump to the nearest neighboring site in the second layer, or it may overcome the barrier $\varepsilon_{\text{barrier}}$ and form a metastable state in the first adlayer that will move practically without barriers. Therefore during the lifetime of the metastable state the local compression of the first layer may move for a long distance, and when the system returns back to the ground state an atom arises in the second layer in a site which may be far away from the initial position of the extra atom. Such an exchange-mediated diffusion should clearly be the favorable diffusion pathway in the case $r_a = 6.3$ because, in this case, the activation barrier for the transition to the metastable state is lower than the activation energy in the second layer, $\varepsilon_{\text{barrier}} < \varepsilon_{\text{act}}$. On the other hand, in the case $r_a = 6.4$ we have the opposite inequality, $\varepsilon_{\text{barrier}} > \varepsilon_{\text{act}}$, and direct jumps to the nearest site of the second layer should be the most probable diffusion path. However, even in this case, transitions to the metastable state may take place and, owing to the high kink mobility, these transitions may lead to a remarkable contribution to the total diffusion coefficient. This aspect is discussed in the following section.

IV. MOLECULAR DYNAMICS SIMULATIONS

The predictions presented above are simply based on static configuration energies and collective dynamical effects

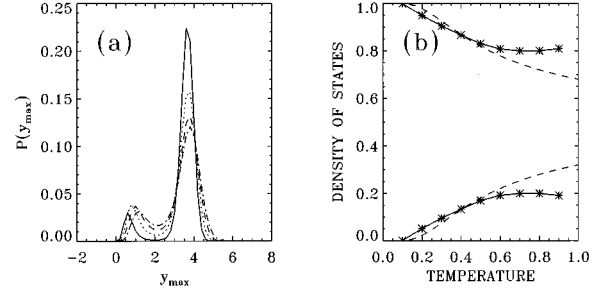


FIG. 5. Simulation results for $r_a = 6.3$ and $\eta = 0.1$. (a) Probability of the maximum of the y position for different temperatures. The solid line corresponds to $T = 0.3$, the dotted line corresponds to $T = 0.5$, the dashed line corresponds to $T = 0.7$, and the dot-dashed line corresponds to $T = 0.9$. (b) Density of states versus temperature. The solid line and stars describe the simulation results, whereas the dashed line corresponds to the estimation (7).

could enter in a nontrivial way to affect the diffusion. Thus these predictions must be checked with full molecular dynamics simulations of the system. Temperature effects are introduced through a standard Langevin approach. The Hamiltonian equation of motion of each atom of mass m is completed by a friction term with a damping coefficient $m\eta$ and a random force with a δ correlation function of factor $2m\eta k_B T$. Starting from the ground state configuration a first time interval t_{th} is allowed to reach the thermal equilibrium state. Then, during a time interval t_{run} we save the dependencies $X(t)$ and $Y(t)$, which define the position of the localized excitation and $y_{\text{max}}(t)$ which defines the maximum y coordinate of the atoms at time t . This last quantity allows us to determine if the system is in the ground state or in the metastable state.

The first step of the analysis has been devoted to the properties of the metastable state at nonzero temperature. In principle, the position Y of the center of mass of the system should tell us whether the system of adatoms is in the ground state or the metastable state. However, in practice, measures of Y do not answer this question because the histogram for the probability $P(Y)$ that Y takes a given value shows only one maximum corresponding to the ground state configuration. This does not mean that the metastable state is never excited, but because of the importance of the fluctuations it is not possible to distinguish the two stable states, characterized by the shift between the two layers of only one atom (among $N = 17$ atoms): the increase of Y is too small. The information on the state of the system can be deduced from y_{max} because this quantity takes a large value if an atom is in the second layer (i.e., when the system is in the ground state). The histogram of the probability $P(y_{\text{max}})$ does exhibit two well-defined maxima corresponding to the ground state and metastable state configurations up to temperatures above $T = 2$ [see Fig. 5(a)]. From this result, it is possible to define an effective free energy of the system as

$$F_{\text{eff}} = -k_B T \ln P(y_{\text{max}}), \quad (5)$$

which is plotted in Fig. 6 at different temperatures. The difference in free energy between the metastable state and the ground state (called ε_{ms} in Sec. III), as well as the height

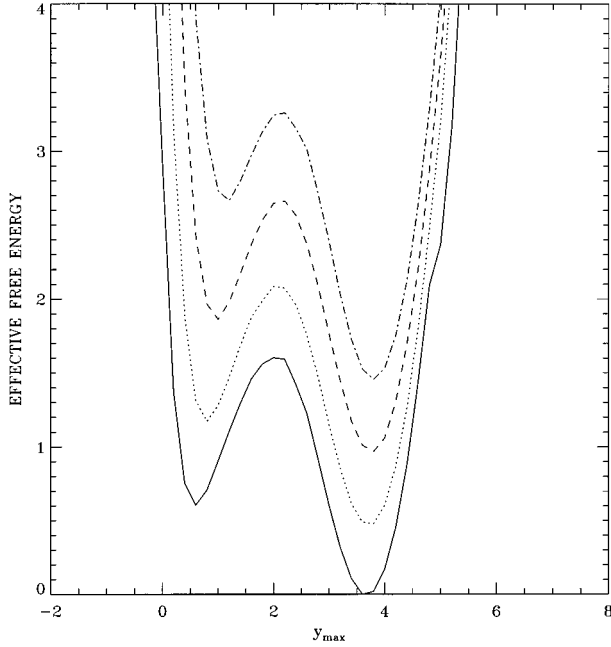


FIG. 6. The effective free energy (ϵ) as function of the maximum of the y atomic positions as follows from the results of Fig. 5. The solid line corresponds to $T=0.3$, the dotted line corresponds to $T=0.5$, the dashed line corresponds to $T=0.7$, and the dot-dashed line corresponds to $T=0.9$.

$\epsilon_{\text{barrier}}$ of the barrier between the ground state and the metastable state, are approximately equal to the values deduced from quasiadiabatic calculations at $T=0$. The relative vertical positions of the curves are not significant, because they depend on the reference in energy that we chose for each temperature. Note, however, that the free energy of the metastable state with respect to the ground state free energy, $\epsilon_{\text{ms}}(T)$, increases with temperature from the value 0.6 at $T=0.3$ to 1.2 at $T=0.9$. This effect may be understood by noticing that the variation of this difference in free energy is related to the entropy of both states as follows:

$$\frac{\partial \epsilon_{\text{ms}}(T)}{\partial T} = \frac{\partial [F_{\text{eff}}(y_{\text{max}}^{\text{ms}}) - F_{\text{eff}}(y_{\text{max}}^{\text{gs}})]}{\partial T} = S_{\text{gs}} - S_{\text{ms}}. \quad (6)$$

Since this variation is positive according to the numerical result, it means that the entropy of the ground state is higher than that of the metastable state. This result is reasonable because the atom isolated in the second layer has more space available to move than when it is in the first layer, and moreover its interaction energy with its neighbors and with the substrate [because of the $\exp(-\gamma'y)$ factor] is weaker.

Integrating the peaks of the histogram of $P(y_{\text{max}})$, we can obtain the occupation numbers of the two states. The density of state for the ground state, ρ_{gs} , is calculated by considering the states on the right of the minimum value between the two peaks. The density of state for the metastable state is then $\rho_{\text{ms}} = 1 - \rho_{\text{gs}}$. In Fig. 5(b) they are shown as functions of the temperature, and compared with the functions

$$\rho_{\text{gs}}^{(0)} = (1 + e^{-\epsilon_{\text{ms}}/k_B T})^{-1} \quad \text{and} \quad \rho_{\text{ms}}^{(0)} = 1 - \rho_{\text{gs}}^{(0)}, \quad (7)$$

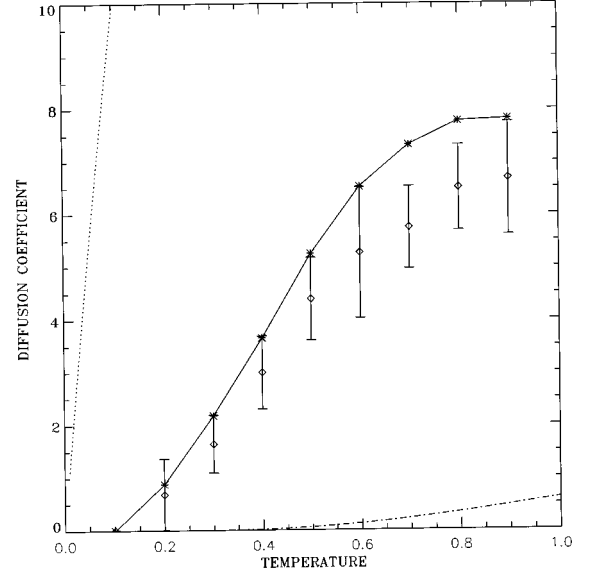


FIG. 7. Diffusion coefficient versus temperature for $r_a = 6.3$ and $\eta = 0.1$. The diamonds correspond to the simulation results. The error bars are computed numerically with 20 simulations. The dotted curve corresponds to D_{kink} and the dash-dotted curve corresponds to D_{act} . The stars and the solid curve describe the estimation result $D = \rho_{\text{gs}} D_{\text{act}} + \rho_{\text{ms}} D_{\text{kink}}$, where ρ_{gs} and ρ_{ms} were taken from the simulation results of Fig. 5(b).

which would be deduced from the quasiadiabatic results without taking into account the variation of the energy of the metastable state with temperature. A significant deviation between the numerical values and the estimation provided by the quasiadiabatic results shows up only in the high temperature range.

The second set of studies has been devoted to a direct determination of the mass diffusion coefficient from the thermalized molecular dynamics simulation. The result is deduced from a series of k simulations at each temperature ($k=20$), each one extending over the time interval t_{run} . From simulation i we extract the diffusion coefficient using

$$D_i = \lim_{t \rightarrow \infty} \frac{\langle [X(t_0 + t) - X(t_0)]^2 \rangle}{2t} \quad (8)$$

(where $t_0 + t$ is lower than t_{run}). Then we average over the k simulations. The results are presented in Figs. 7 and 8, and discussed in the following section.

Besides the total diffusion coefficient, we calculate also the kink diffusion coefficient (i.e., the diffusion coefficient of the system in the metastable state). For this, we start from the metastable state and monitor the maximum y_{max} coordinate of the atoms: when an atom escapes from the first adlayer, we stop the run. A reliable numerical estimation of the kink diffusion coefficient is only possible at low temperature when the metastable state has a sufficient lifetime. The results are presented in Fig. 9.

V. DISCUSSION

Let us now come to the main point, an analytical estimate of the role of kinks in the process of surface diffusion. As shown above, the system may evolve from one gs configu-

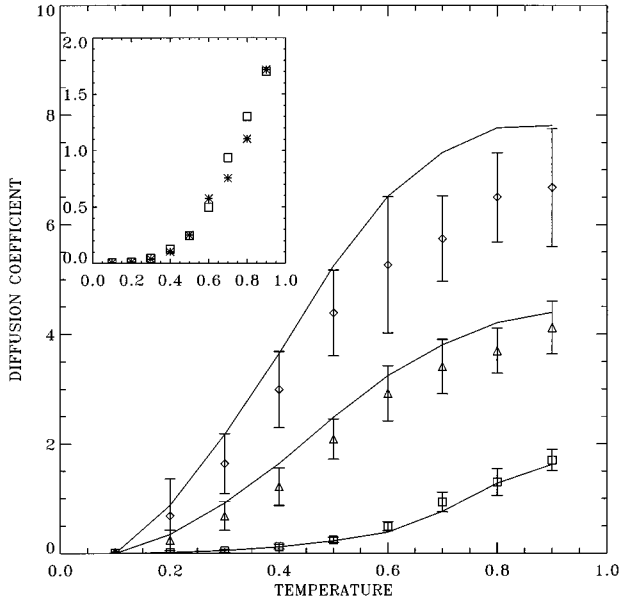


FIG. 8. Comparison between the MD results and the theoretical values of the diffusion coefficient in four cases. The symbols correspond to the simulation results, and the solid curves to the theoretical ones. The diamonds describe the case $r_a=6.3$ and $\eta=0.1$, the triangles, the case $r_a=6.3$ and $\eta=0.3$, the squares correspond to the case $r_a=6.4$ and $\eta=0.1$, and the stars, to the case $r_a=6.4$ and $\eta=0.3$.

ration to an another gs configuration with the atom occupying a neighboring site in the second adlayer by two pathways, either by a direct atomic jump over the barrier ε_{act} or through a two-stage mechanism involving the metastable state in the first adlayer. For such a two-way process the total diffusion coefficient can be calculated by the method described by Kutner and Sosnowska.¹¹ The result is trivial:

$$D = \rho_{\text{gs}} D_{\text{act}} + \rho_{\text{ms}} D_{\text{kink}}, \quad (9)$$

where the occupation numbers ρ_{gs} and ρ_{ms} were defined above.

The hopping diffusion coefficient D_{act} may be estimated with the help of the seminal result of the Kramers theory¹²

$$D_{\text{act}} \approx \left(\sqrt{\omega_b^2 + \frac{\eta^2}{4}} - \frac{\eta}{2} \right) \frac{\omega^* a_s^2}{\omega_b 2\pi} \exp\left(-\frac{\varepsilon_{\text{act}}}{k_B T}\right), \quad (10)$$

where ω^* (ω_b) is the frequency of the linearized oscillations of the system near the ground (unstable) state. As shown on Fig. 2, the potential energy for the motion over the barrier is well approximated by a sinusoidal function $V(x) = \varepsilon_{\text{act}}[1 + \cos(2\pi x/a_s)]/2$, so that $\omega^* = \omega_b = \sqrt{\varepsilon_{\text{act}}/2m}$. Finally, as $a_s = 2\pi$ and $m = 1$ with our units, we get

$$D_{\text{act}} \approx \left(\sqrt{\frac{\varepsilon_{\text{act}}}{2} + \frac{\eta^2}{4}} - \frac{\eta}{2} \right) 2\pi \exp\left(-\frac{\varepsilon_{\text{act}}}{k_B T}\right). \quad (11)$$

To estimate the diffusion coefficient D_{kink} of the metastable state, recall that the atom inserted into the chain creates a local distortion that can be considered as a kink in the Frenkel-Kontorova model. In the continuum approximation the equation of motion reduces to the exactly integrable sine-

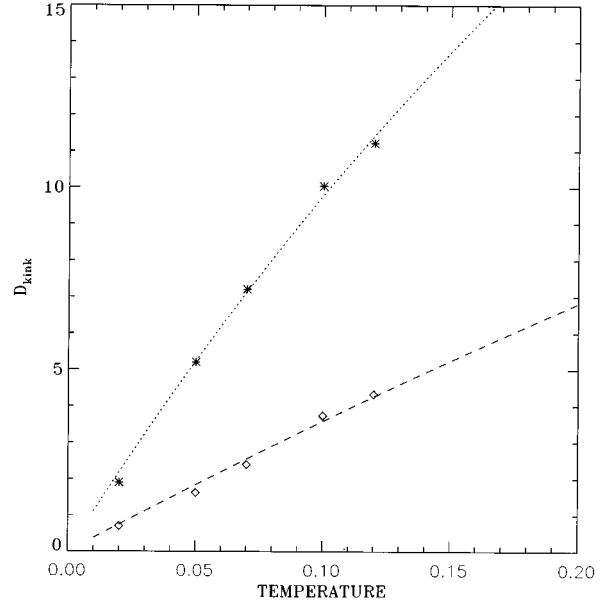


FIG. 9. The kink diffusion coefficient versus temperature for $r_a=6.3$. The symbols correspond to the simulation results and the lines describe the estimated results of Eq. (15). The stars and the dotted curve correspond to $\eta=0.1$, the diamonds and the dashed curve, to $\eta=0.3$. The parameters m_{kink} and α were obtained by fitting the expression (15) to the simulation data for the case $\eta=0.1$, and then the same values were used for $\eta=0.3$.

Gordon (SG) equation. This limit, in which a defect would propagate freely as a soliton in the system, can be used as a starting point for a perturbative analysis of the influence of the discreteness of the lattice. When the continuous translational invariance is broken, one finds that the kink experiences a periodic potential, with the periodicity of the lattice, which is known as the Peierls-Nabarro barrier in dislocation theory. A precise evaluation of the PN barrier turns out to involve subtle effects, particularly when discreteness effects are weak,¹³ but a recent analysis has derived accurate results in this case.¹⁴ The basic result is that the shape of the kink can be obtained by solving a Klein-Gordon equation obtained by replacing the actual substrate potential $V(x)$ by an effective potential

$$V_{\text{eff}}(x) = V(x) - \frac{1}{24g} [V'(x)]^2 \quad (12)$$

where $g = a_s^2 V''_{\text{int}}(a_s)/(2\pi^2 \varepsilon_s) = V''_{\text{int}}(a_s)$ is the elastic constant of the atomic chain. This expression allows us to derive the value of the mass of the kink, which is given by the general expression for a Klein-Gordon model,

$$m_{\text{kink}} = \frac{m}{a_s^2 \sqrt{g}} \int_0^{a_s} \sqrt{2V_{\text{eff}}(x)} dx. \quad (13)$$

This formula gives the usual expression $m_{\text{kink}} = 8m/(a_s^2 \sqrt{g})$ in the sine-Gordon case if, instead of the effective potential, we use the actual potential $V(x) = [1 - \cos(2\pi x/a_s)]$. For the values of g which are obtained with our parameters (see Table II), the correction to the SG value due to discreteness

TABLE II. Parameters corresponding to the kink (metastable state): g is the elastic constant, m_{kink} is the kink mass, and $\varepsilon_{\text{PN}}(\text{theory})$ is the amplitude of the Peierls-Nabarro barrier.

Parameter	$r_a=6.3$	$r_a=6.4$
g	2.243	2.759
m_{kink}	0.1344	0.1214
$\varepsilon_{\text{PN}}(\text{theory})$	1.22×10^{-3}	2.98×10^{-4}

is small, giving, for instance, $m_{\text{kink}} = 7.95m/(a_s^2\sqrt{g})$ for the case $r_a=6.3$. The proper treatment of discreteness is much more important for the evaluation of the amplitude of the Peierls potential which is obtained as¹⁴

$$\varepsilon_{\text{PN}} \approx 712.26\varepsilon_s g \exp(-\pi^2\sqrt{g}). \quad (14)$$

Table II gives the values of g , m_{kink} , and ε_{PN} which result from the interaction potential (4) with $r_a=6.3$ and $r_a=6.4$. It shows that the amplitude of the PN potential is negligible with respect to the barrier ε_{act} corresponding to the translation of the extra atom in the second layer. This is in agreement with the numerical results of Sec. III. Moreover, this value $\varepsilon_{\text{PN}} \ll k_B T$ at the temperature that we consider shows that the kink motion is not thermally activated. Its diffusion coefficient can be derived from the formula for a free diffusion,

$$D_{\text{kink}} = \frac{k_B T}{m_{\text{kink}} \eta_{\text{kink}}}, \quad (15)$$

where η_{kink} is an effective viscous friction for kink motion. At $T=0$ η_{kink} is simply given by $\eta_{\text{kink}} \approx \eta$, where η is the viscous friction for the motion of an isolated adatom due to energy exchange with the substrate. The value of η is usually¹⁵ about $\eta \sim \omega_0/10$. But at nonzero temperature η_{kink} depends on T because of the coupling of the lattice phonons with the highly nonlinear core of the kink. The simplest form for this dependence is¹⁶

$$\eta_{\text{kink}} \approx \eta + \alpha T, \quad (16)$$

where α is a coefficient which cannot be obtained analytically but could be obtained experimentally, as in the case of copper.¹⁷

In our analysis, we treat m_{kink} and α as adjustable parameters. They are chosen by fitting with Eq. (15) the temperature evolution of D_{kink} determined by the MD simulations with $\eta=0.1$ and $r_a=6.3$. The parameters $m_{\text{kink}}=0.0886$ and $\alpha=0.155$ obtained in this particular case are also valid for the case $\eta=0.3$ as shown from Fig. 9. Moreover, the expression (15) with the *same* parameters describes the simulation results for the diffusion in the first adlayer for the case $r_a=6.4$ as well. This rather good agreement between the numerical results and the analytical estimation of D_{kink} shows that, although the SG description may seem rather crude for the generalized FK model, it provides a good basis for analysis. This is confirmed by the comparison between the fitted value of m_{kink} and the theoretical value given by Eq. (13): the fitted value is smaller than the theoretical one, but the order of magnitude of m_{kink} is nevertheless correctly given by the discrete SG calculation.

Having obtained analytical estimates for the two diffusion coefficients D_{act} and D_{kink} , we are now in a position to estimate the role of the kink diffusion in the general process of atomic diffusion in the adsorbed layer. The role of both mechanisms is well illustrated on Fig. 7. First, one can observe that the temperature dependence of the total diffusion coefficient D deduced from the MD simulations is well reproduced by Eq. (9). It should be noticed that at this level the fit is obtained *without* adjustable parameters, since our parameters have been deduced from the study of D_{kink} alone and the densities of states ρ_{gs} and ρ_{ms} are the measured quantities. The good agreement points out that the diffusion mechanism that we propose, involving two different processes, provides a correct description of diffusion as it can be observed in MD simulations of the generalized FK model. It is also important to notice that *both mechanisms* are essential to reproduce the numerical results. If one considered only one of the two processes, i.e., assumed that $\rho_{\text{gs}}=1$ or $\rho_{\text{ms}}=1$, the diffusion coefficient would evolve versus T along the dash-dotted or dotted line of Fig. 7. The theoretical value of D would disagree completely with the MD results.

Figure 8 summarizes the results by providing a comparison between the temperature dependence of D observed by MD and the theoretical value of Eq. (9) for $r_a=6.3$ and $r_a=6.4$ and two values of the damping coefficient η . This figure shows that all the numerical results are well described by the two-process diffusion with only two adjustable parameters α and m_{kink} . The results show also that, even in the case $r_a=6.4$, for which direct jumps to the nearest adsite in the second layer have to overcome a much lower barrier than the barrier for the transition to the metastable state, the solitonic-exchange mechanism involving the metastable state still brings a crucial contribution to the total diffusion coefficient D . This is due to the extremely high mobility of the metastable state.

VI. CONCLUSION

Following our results, one can distinguish three different diffusion mechanisms for atoms adsorbed on a crystalline surface.

The first one is the *conventional diffusion* (sometimes called hopping diffusion) which involves only one atomic layer. It can be an individual process when an adatom directly jumps from one adsorption site to the nearest adsite. The diffusion coefficient in this case follows the Arrhenius law $D(T) = A \exp(-\varepsilon_{\text{act}}/k_B T)$ with the preexponential factor being independent of (or weakly dependent on) T . At high coverages $\theta \lesssim 1$ (as well as for $\theta \lesssim 2$, etc.) owing to the interaction between the adatoms, the activation energy ε_{act} decreases with respect to the height of the original substrate potential ε_s . For a strong interatomic interaction the motion takes a collective (concerted) character and may be described with the help of the kink concept.^{9,4} In this case the activation energy ε_{act} for the chemical diffusion becomes the Peierls-Nabarro barrier ε_{PN} , which is significantly lower than the individual activation energy. Therefore the process is generally no longer thermally activated and $D(T)$ is approximately given by the free diffusion formula $D(T) \approx k_B T / m_{\text{kink}} \eta_{\text{kink}}$.

While for the conventional diffusion the underlying ada-

toms in the first adlayer play a passive role, creating the effective external potential for the diffusion of atoms in the second adlayer, for the *exchange diffusion* mechanism this role becomes active. Two types of mechanisms can be considered. The “conventional” (or “one-step”) exchange diffusion mechanism has been known for a long time. It occurs when an adatom A from the second layer “pushes out” an adatom B from its regular position in the first adlayer and occupies the free site so created. The new configuration has only a single adatom (B) in the second adlayer. The intermediate configuration with both adatoms A and B inserted into the first adlayer is unstable. It corresponds to a saddle point in the potential energy surface. The elementary diffusion step takes a short time, $\sim 10^{-13}$ sec. The diffusion coefficient for the one-step exchange mechanism should follow the same Arrhenius law as for the conventional hopping diffusion with the activation energy corresponding to the saddle state. Exchange diffusion may be important for coverages $\theta \geq 1$, when the first adlayer is complete and the second one starts to grow.

The diffusion mechanism studied in the present work is a *two-step exchange* diffusion mechanism. The main difference from one-step exchange diffusion is that the configuration with the adatom inserted into the first adlayer, now corresponds to a *metastable* state instead of the unstable (saddle) state. Because this metastable state corresponds to a kink configuration which is characterized by a very high mobility, the mechanism may be called the “exchange-solitonic” mechanism of surface diffusion. For this mechanism the diffusion follows an Arrhenius law too, but now the activation energy corresponds to the difference in energies between the metastable state and the ground state (and not to

the barrier for the transition from the second adlayer to the first one), while the preexponential factor is determined by the kink diffusion coefficient and essentially depends on temperature. The mass diffusion coefficient in this situation is described by the expression (9) where D_{act} and D_{kink} are given by Eqs. (11) and (15).

We considered above the situation where an atom is diffusing in the second adlayer over a filled first adlayer. It is clear that the same situation can occur for adatoms of the first layer when the adatoms are the same as the atoms of the substrate. Indeed, in this case the top-layer substrate atoms play the same role as that of the first-layer adatoms in the former case. In particular, the exchange diffusion mechanism was observed when de Lorenzi and Jacucci¹⁸ investigated by the MD method the self-diffusion of Na atoms adsorbed on the surface of a Na metal crystal. They found that the exchange mechanism is responsible for the diffusion across the rows on the furrowed crystal surface. This conclusion was later confirmed by the field ion microscope technique for the diffusion of atoms adsorbed on transition metal surfaces.^{1,2}

It seems possible and would be interesting to find and investigate the exchange-solitonic mechanism of surface diffusion experimentally with the field-ion microscope or scanning tunneling microscope technique. It may be predicted that such a diffusion is to be expected for coverages $\theta \sim a_s/r_a$.

ACKNOWLEDGMENTS

The authors thank Thierry Cretegy for helpful discussions. Part of this work has been supported by the NATO Grant No. LG920236.

*Permanent address: Institute of Physics, Ukrainian Academy of Sciences, 46 Science Avenue, UA-252022 Kiev, Ukraine.

† Electronic address: tdauxois@physique.ens-lyon.fr

¹A. Zangwill, *Physics at Surfaces* (Cambridge University Press, Cambridge, England, 1988).

²G. Ehrlich and K. Stolt, *Annu. Rev. Phys. Chem.* **31**, 603 (1980); A. G. Naumovets and Yu. S. Vedula, *Surf. Sci. Rep.* **4**, 365 (1985); J. D. Doll and A. F. Voter, *Annu. Rev. Phys. Chem.* **38**, 413 (1987); R. Gomer, *Rep. Prog. Phys.* **53**, 917 (1990).

³V. K. Medvedev, A. G. Naumovets, and T. P. Smereka, *Surf. Sci.* **34**, 368 (1973); M. S. Gupalo, V. K. Medvedev, B. M. Palyukh, and T. P. Smereka, *Sov. Phys. Solid State* **21**, 568 (1979).

⁴O. M. Braun and Yu. S. Kivshar, *Phys. Rev. B* **50**, 13 388 (1994).

⁵J. E. Black and Zeng-Ju Tian, *Phys. Rev. Lett.* **71**, 2445 (1993).

⁶O. M. Braun and M. Peyrard, *Phys. Rev. B* **51**, 17 158 (1995).

⁷M. Peyrard and M. Remoissenet, *Phys. Rev. B* **26**, 2886 (1982).

⁸O. M. Braun and E. A. Pashitsky, *Poverkhn. Phys. Himiya Mehan. (USSR)* No. 7, 49 (1984) [*Phys. Chem. Mech. Surf.*

(U.K.) **3**, 1989 (1985)].

⁹O. M. Braun, Yu. S. Kivshar, and I. I. Zelenskaya, *Phys. Rev. B* **41**, 7118 (1990).

¹⁰O. M. Braun and V. K. Medvedev, *Usp. Fiz. Nauk* **157**, 631 (1989) [*Sov. Phys. Usp.* **32**, 328 (1989)].

¹¹R. Kutner and I. Sosnowska, *Acta Phys. Pol. A* **47**, 475 (1975); *J. Phys. Chem. Solids* **38**, 741 (1977).

¹²P. Hänggi, P. Talkner, and M. Borkovec, *Rev. Mod. Phys.* **62**, 251 (1990).

¹³S. Flach and C. Willis, *Phys. Rev. E* **47**, 4447 (1993).

¹⁴S. Flach and K. Kladko (unpublished).

¹⁵O. M. Braun, A. I. Volokitin, and V. P. Zhdanov, *Usp. Fiz. Nauk* **158**, 421 (1989) [*Sov. Phys. Usp.* **32**, 605 (1989)].

¹⁶F. Marchesoni, *Phys. Rev. Lett.* **73**, 2394 (1994); A. D. Brailsford, *J. Appl. Phys.* **43**, 1380 (1972).

¹⁷G. A. Alers and D. O. Thompson, *J. Appl. Phys.* **32**, 283 (1961).

¹⁸G. de Lorenzi and G. Jacucci, *Surf. Sci.* **164**, 526 (1985).